Icarus 226 (2013) 355–363

Contents lists available at SciVerse ScienceDirect

Icarus

journal homepage: www.elsevier.com/locate/icarus

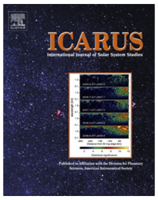

Influence of NaCl on ice VI and ice VII melting curves up to 6 GPa, implications for large icy moons

B. Journaux *, I. Daniel, R. Caracas, G. Montagnac, H. Cardon

Laboratoire de Géologie de Lyon – Terre, Planètes, Environnement, UMR 5276, CNRS, École Normale Supérieure de Lyon, Université Claude Bernard Lyon 1, 2 rue Raphael Dubois, 69622 Villeurbanne cedex, France

ARTICLE INFO

Article history:
Received 30 October 2012
Revised 24 May 2013
Accepted 28 May 2013
Available online 13 June 2013

Keywords:
Ices
Satellites, Composition
Experimental techniques
Ganymede
Exobiology

ABSTRACT

The influence of sodium chloride salt on the liquidus of ice VI and ice VII has been measured for concentrations ranging between 0.01 and 4 mol kg^{-1} NaCl. Dissolved NaCl significantly increases the melting pressure or decreases the melting temperature as a function of the salt concentration and induces a density crossover between ice VI and the brine. For NaCl concentrations higher than 2.5 mol kg^{-1} ice VI is more buoyant than the brine. The liquidus points are fitted to a second order polynomial law and a model is provided to predict the melting pressures of ice VI and ice VII ($P_{m,VI}$ and $P_{m,VII}$), respectively as a function of temperature T (K) and NaCl concentration X_{NaCl} (mol kg^{-1}):

$$\begin{aligned}P_{m,VI}(T,X_{NaCl}) = {} & 9.27 + 0.996X_{NaCl} - (6.99\times10^{-2} + 7.6\times10^{-3}X_{NaCl})\cdot T \\ & + (1.414\times10^{-4} + 1.541\times10^{-5}X_{NaCl})\cdot T^2\end{aligned}$$

$$\begin{aligned}P_{m,VII}(T,X_{NaCl}) = {} & -0.133 + 0.122X_{NaCl} - (1.28\times10^{-4} + 4.17\times10^{-4}X_{NaCl})\cdot T \\ & + (1.86\times10^{-5} + 8.56\times10^{-7}X_{NaCl})\cdot T^2\end{aligned}$$

The temperature of the triple point between ice VI, ice VII and the brine shifts of -7 K/X_{NaCl} along the 2.17 GPa isobar. The consequences of potentially dissolved NaCl for the internal structure of water rich planetary bodies are discussed. The density crossover between ice VI and brines suggests that migration of brines through a deep ice VI layer is enhanced for high thermal profiles and is unlikely for colder thermal conditions. It also suggests that patches of brines may actually be gravitationally stable at the interface between the bedrock and a deep ice VI basal layer allowing for a potential new class of exobiological habitat.

1. Introduction

Water is considered as a prerequisite for life including extraterrestrial life. Liquid H_2O as a solvent has peculiar physical and chemical properties, among which a large dipole moment allowing stabilization of large organic molecules and complex carbon chemistry (see review by Lammer et al. (2009)). In stellar systems, the habitable zone is defined by the potential presence of liquid water at the surface of planetary bodies (Kasting et al., 1993). Nevertheless stable liquid H_2O may be found in some planetary environments far beyond the snow line (Lammer et al., 2009). In particular, the presence of a deep ocean has been hypothesized in water rich planetary bodies such as the Galilean satellites Europa, Callisto and Ganymede, assuming a thermal gradient high enough to reach the melting of ice at depth. The interior of these bodies may host a suite of the high-pressure (HP) solid phases of H_2O like ice III, V, VI, VII (Fortes and Choukroun, 2010) and eventually liquid water between crustal ice Ih and deeper dense ice phases if the surface temperature is high enough. The classification of habitats proposed for planetary oceanic environment mainly relies on the location of liquid H_2O at depth (Lammer et al., 2009). Class III habitats are characterized by deep oceans, which interact with mantle or core silicates. Geochemical exchanges by aqueous alteration or hydrothermal reactions between aqueous fluids and the rocky substrate could then provide nutrient and energy for a putative extraterrestrial life. In class IV habitats, melting of dense ice would occur within the H_2O rich layer and HP ices would then be present between the liquid ocean and the bedrock. Such an icy substrate would certainly limit geochemical exchanges and consequently the habitability of the overlying ocean. Water-rich planetary bodies also include the recently detected extra-solar “ocean planets” (Kuchner, 2003; Léger et al., 2004) like Kepler-11b (Lissauer et al., 2011), GJ-581d (Udry et al., 2007) and GJ-1214b (Charbonneau et al., 2009). In the latter very large planets, pressure is

---

* Corresponding author.
E-mail address: baptiste.journaux@ens-lyon.fr (B. Journaux).

0019-1035/$ - see front matter © 2013 Elsevier Inc. All rights reserved.
http://dx.doi.org/10.1016/j.icarus.2013.05.039

very high at depth and the large H_2O mantle consists mostly in the dense ice VII and ice X (Sotin and Grasset, 2007; Fu et al., 2010). Depending on the thermal gradient, a 50–100 km thin liquid class IV ocean may occur at the top of this mantle.

Astrophysical and geophysical modeling of water rich bodies (e.g. Sotin and Grasset, 2007; Tobie et al., 2008; Fu et al., 2010; Schubert et al., 2010; Castillo-Rogez and Lunine, 2010) mostly stands to date on the phase diagram of pure H_2O. Only a few studies take into account the properties of the binaries between H_2O and other solutes to infer the internal structure of those planetary bodies. The compounds of interest include for instance ammonia and/or methane (Lunine and Stevenson, 1987; Grasset and Pargamin, 2005; Choukroun and Grasset, 2007, 2010; Choukroun et al., 2010; Fortes, 2012). However the role of salts in the geodynamics of water-rich bodies has received much less attention despite observations and experimental data since the early 1930s (Adams and Gibson, 1930; Adams, 1931). Among salts, sulfates have been reported in carbonaceous chondrites (Fredriksson and Kerridge, 1988), observed at the surface of Europa (McCord et al., 1998; Carlson et al., 2009), and predicted from modeling water–rock interactions (e.g. Zolotov and Kargel, 2009). Consequently, the investigation of the $MgSO_4$–H_2O binary has been of interest to many authors who have clarified the stability of $MgSO_4$ sulfate hydrates under a variety of pressure (P) and temperature (T) conditions (Hogenboom et al., 1995; Fortes and Choukroun, 2010; Nakamura and Ohtani, 2011) as well as the influence of these phases on the internal structure of Ganymede (Vance et al., 2013). The remote spectroscopic detection in the near infrared of chloride salts being more challenging at the surface of icy bodies, but in the form of hydrohalite $NaCl{\cdot}2H_2O$, their investigation in planetary sciences is more limited. The plausible abundance of salt in the H_2O rich bodies is supported by Galileo probe magnetometer observations suggesting the presence of dissolved salt inside a deep and large liquid reservoir in the depths of Europa, Callisto and Ganymede (Khurana et al., 1998; Sohl et al., 2010; Kivelson and Khurana, 2002). Recent Cassini flybys of Enceladus pointed out the sodium rich composition of the active polar plumes (Postberg et al., 2011). During the early evolution of such H_2O rich bodies, aqueous fluids and/or ice have probably reacted with chondritic material collected during the accretion stage certainly producing alkaline fluids with Na^+ and Cl^- ions as the major species (Zolotov, 2012). Altogether these observations suggest that chloride salts may actually be widespread in planetary aqueous interiors and should be considered when modeling the internal structure, the evolution and dynamics of the H_2O rich planetary bodies. This has been investigated very early on with the pioneering experiments to 1.2 GPa by Adams (1931). The NaCl–H_2O binary has also received interest from the fluid inclusion community interested in relatively moderate pressure and high temperature compared to the P–T conditions inside icy bodies (e.g. Chou, 1987; Driesner and Heinrich, 2007). More recently a series of experimental work focused on the P–T range suitable for the interior of icy moons. Frank et al. (2008) showed that the phase relation in the NaCl–H_2O binary at high pressure might actually change the internal structure of a hypothetical H_2O-rich planet.

Any change in the melting temperature or pressure of the dense ices may also alter the shape of the impact craters observed on icy surfaces. Impact craters on icy surfaces are slightly different from their counterparts on rocky surfaces (Senft and Stewart, 2011 and references therein). They are characterized by a shallow depth and by the occurrence of central pits or central domes. Formation of these unique morphologies is tentatively explained by the presence of an underlying liquid ocean and by the transformation of liquid H_2O into dense ice VI and ice VII during impact and by the stiffness of the latter high-pressure phases (Schenk, 2002; Senft and Stewart, 2011). Taking into account the alteration of the melting curves of ice VI and ice VII when NaCl is added to the system may actually change the characteristic morphologies of the impact crater on the icy surface of Callisto or Europa for instance.

Here we present accurate experimental data in the NaCl–H_2O binary for the evolution of the melting curve of ice VI and ice VII as a function of the salinity of the fluid. This extends the pioneering study by Adams (1931) on the melting curves of ice VI in the NaCl–H_2O binary, the results by Frank et al. (2008, 2013) on ice VII and the data at low temperature by Valenti et al. (2012).

2. Experimental methods

Experiments were performed in a gas membrane diamond-anvil cell (DAC) (Chervin et al., 1995) equipped with ultra-low fluorescence diamond anvils of 0.5 mm culet. The DAC was externally heated by a resistive sleeve and thermally insulated with ceramic fiber tape for a high thermal stability. At the highest temperature, the stability was better than ±0.5 K. Temperature was read from a commercially calibrated K-type thermocouple glued on the side of one anvil in contact with the gasket. Under such experimental conditions, no detectable temperature difference has ever been measured between the pressure chamber and the side of the diamond, thanks to the high thermal conductivity of diamond. As a pressure chamber, we used a stainless steel gasket indented at 70 μm thickness drilled with a 200 μm hole and lined with platinum to avoid reaction between the aqueous fluid and the gasket. Ruby spheres of 10 μm diameter located into the experimental fluid volume, served as a pressure gauge. Neither dissolution nor alteration of the ruby spheres was observed over the temperature and pressure range of the present work. Ruby spheres were from a single batch. They were doped with 3600 ppm of Cr^{3+} and annealed long enough to avoid internal strain (Chervin et al., 2001). Pressure was calculated from the shift of the R1 fluorescence line after its temperature-induced shift was taken into account (Mao et al., 1986; Datchi et al., 2007). The evolution of the R1 shift with temperature was calibrated for the present batch of ruby spheres over the temperature range relevant to the present study. The data are best fitted to a second order polynomial:

$$\nu_{R1} = x_1 + x_2 \cdot (T - 273.15) + x_3 \cdot (T - 273.15)^2 \tag{1}$$

with ν_{R1} the wavenumber of the R1 fluorescence line (cm^{-1}), T the temperature (K) and $x_1 = 14407.1\ cm^{-1}$ ($\sigma_{x_1} = 0.045$), $x_2 = 0.1376\ cm^{-1}\ K^{-1}$ ($\sigma_{x_2} = 7.32 \times 10^{-4}$) and $x_3 = 8.1417 \times 10^{-5}\ cm^{-2}\ K^{-2}$ ($\sigma_{x_3} = 2.36 \times 10^{-6}$) the the polynomial coefficients and their associated standard errors. The overall uncertainty on pressure is therefore always better than 76 MPa.

Ice phases were identified by optical microscopy combined with Raman spectroscopy. Representative spectra of ice VI, ice VII and of the liquid phase collected during the experiments are displayed in Fig. 1. Raman and fluorescence spectra were collected in the backscattered geometry using the 514.5 nm line of an Ar^+ laser (Spectra Physics™) as the incident energy. A LabRam HR800 Raman spectrometer (Jobin Yvon Horiba™) equipped with a 600 g/mm grating and a Mitutoyo™ long-working distance 50× objective. The neon emission lines from a Ne-lamp were collected simultaneously to the fluorescence and Raman spectra to obtain the most accurate measurements. A more precise description of this setup is available in Facq et al. (2013).

The salty solutions were prepared by dissolving sodium chloride (99.99% ultra pure sodium chloride, Aldrich™) into ultra pure water (Milli-Q™). Solutions with four different molalities of 0.01, 1.0, 2.5 and 4.0 mol kg^{-1} were obtained by quickly weighting the appropriate mass of sodium chloride dried for 6 h at 400 K prior to dissolution. Before loading, the solutions and the DAC were kept at 278 K to prevent evaporation during loading. A droplet of the